RESEARCH ARTICLE

K. Thomson · D. Hutton

Geometry and growth of sill complexes: insights using 3D seismic from the North Rockall Trough

Abstract Doleritic sill complexes, which are an important component of volcanic continental margins, can be imaged using 3D seismic reflection data. This allows unprecedented access to the complete 3D geometry of the bodies and an opportunity to test classic sill emplacement models. The doleritic sills associated with basaltic volcanism in the North Rockall Trough occur in two forms. Radially symmetrical sill complexes consist of a saucer-like inner sill at the base with an arcuate inclined sheet connecting it to a gently inclined, commonly ragged, outer rim. Bilaterally symmetrical sill complexes are sourced by magma diverted from a magma conduit feeding an overlying volcano. With an elongate, concave upwards, trough-like geometry bilaterally symmetrical sills climb away from the magma source from which they originate. Both sill complex types can appear as isolated bodies but commonly occur in close proximity and consequently merge, producing hybrid sill complexes. Radial sill complexes consist of a series of radiating primary flow units. With dimensions up to 3 km, each primary flow unit rises from the inner saucer and is fed by primary magma tube. Primary flow units contain secondary flow units with dimensions up to 2 km, each being fed by a secondary magma tube branching from the primary magma tube. Secondary flow units in turn are composed of 100-m scale tertiary flow units. A similar branching hierarchy of flow units can also be seen in bilaterally symmetrical sill complexes, with their internal architecture resembling an enlarged version of a primary flow unit from a radial sill complex. This branching flow pattern, as well as the interaction between flow units of varying orders, provides new insights into the origin of the structures commonly seen within sill complexes and

the hybrid sill bodies produced by their merger. The data demonstrate that each radially symmetrical sill complex is independently fed from a source located beneath the centre of the inner saucer, grows by climbing from the centre outwards and that peripheral dyking from the upper surface is a common feature. These features suggest a laccolith emplacement style involving peripheral fracturing and dyking during inner saucer growth and thickening. The branching hierarchy of flow units within bilaterally symmetrical sill complexes is broadly similar to that of primary flow units within a radially symmetrical sill complex, suggesting that the general features of the laccolith emplacement model also apply.

Keywords Sill intrusion · Sill emplacement models · Magma flow units · 3D seismic · North Rockall Trough · Volcanic continental margins

Introduction

Volcanic continental margins, such as those along the Atlantic margin of north-western Europe, are characterised by the voluminous production of basaltic magma during the break-up process (White and McKenzie 1989). This magma can typically be subdivided between the magmatic underplate beneath the continental margin and the overplate consisting of both extrusive volcanics and shallow, upper crustal, intrusives (White 1988). Although extrusive volcanism in such settings is reasonably well understood (e.g. Upton 1988; Musset et al. 1988), our understanding of the contemporaneous intrusive component (sills and dykes) is more limited. In particular, a number of models have been proposed to account for the geometries, and growth histories of sills (Bradley 1965; Burger et al. 1981; Francis 1982; Chevalier and Woodford 1999) but the systematic testing of such models has been limited by several key problems. Crucial to validating models for the emplacement of sills is a detailed understanding of their complete geometry and their growth histories. Even in classic outcrop examples (e.g.

K. Thomson (✉) · D. Hutton
School of Geography, Earth and Environmental Sciences,
University of Birmingham, Edgbaston,
Birmingham, 15 2TT, UK
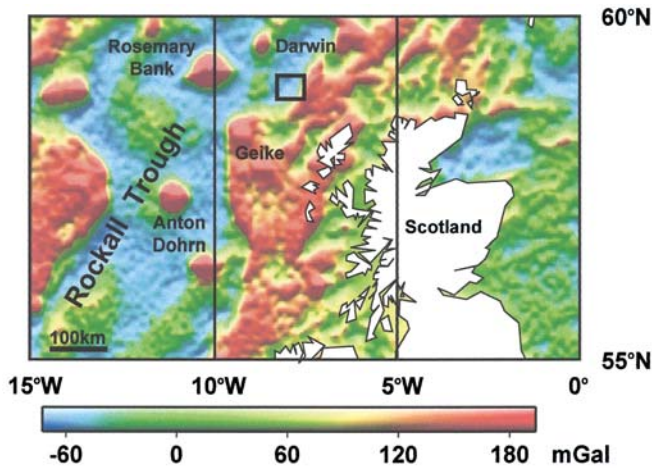e-mail: k.thomson@bham.ac.uk
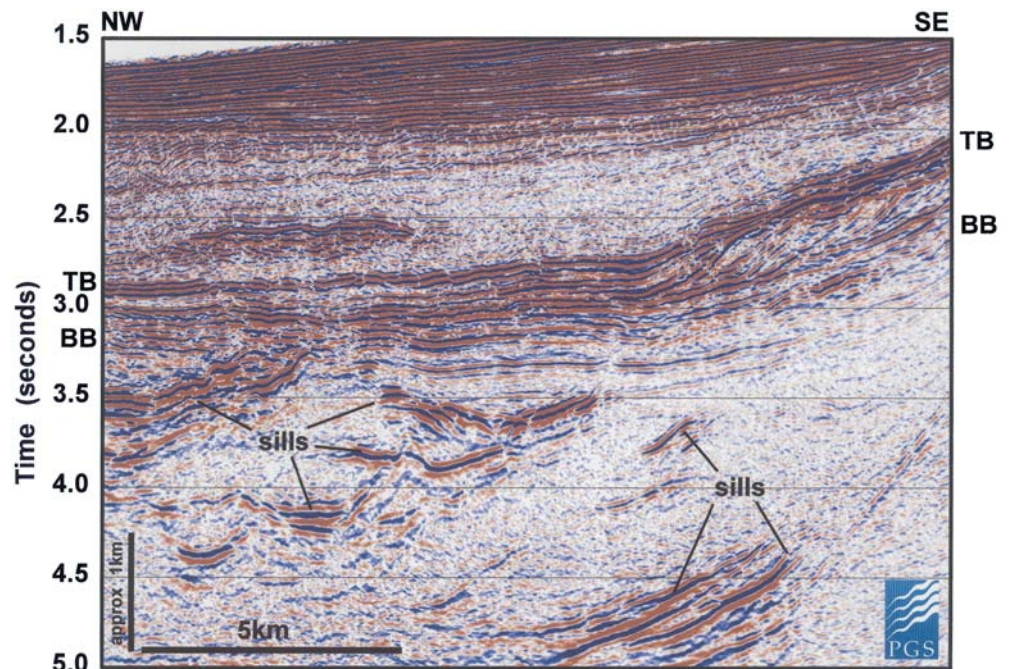Tel.: +44-121-4144942
Fax: +44-121-4146156

Fig. 1 Bouger gravity map showing the location of the Rockall Trough, and some of the major igneous centres. The *rectangle* marks the approximate position of the 3D seismic dataset used in this study

datasets allow the accurate and complete description of sill geometries at a level of detail comparable to many outcrop based studies. In addition, advances in seismic volume visualisation allow features relatable to magma flow directions and sill complex growth to be observed. Using 3D seismic data from the North Rockall Trough (Fig. 1), this paper will examine the geometries of sill complexes in volcanic margin settings, the magma flow patterns within such bodies, and hence sill growth histories and their relationships to volcanic features. Seismic-scale structures indicative of magma flow directions will also be identified and models for sill emplacement discussed.

The Rockall Trough: a geological summary

Underlying the present-day deep-water basin of the same name, the Rockall Trough is a north to north-easterly-trending sedimentary basin that forms part of the 'proto-North Atlantic' rift zone (Smythe 1989). The Trough contains a Mesozoic to present-day sedimentary succession that overlies Precambrian Lewisian amphibolite gneisses (Tate et al. 1999). Details of the depositional history are sparse due to the limited number of exploration wells drilled in the region and their limited depths of penetration. However, sedimentation has occurred in a range of terrestrial and shallow to deep marine environments with the available data summarised in Tate et al. (1999). Extensive magmatic activity occurred in the basin, with lavas being erupted from at least the latest Cretaceous until the early Eocene (Fig. 2; Mussett et al. 1988; Upton 1988; Hitchen and Ritchie 1993). This was associated with the emplacement of large igneous centres along the basin axis (Anton Dohrn, Rosemary Bank,

the Karoo sills of South Africa; Du Toit 1920) the amount of 3D structural information is limited by the available exposure and consequently the true 3D complexity in such areas can, in many cases, be underestimated. Furthermore, the quantification of magma flow directions, traditionally achieved through a combination of geometric features, magmatic and magnetic fabrics within such bodies (e.g. Rickwood 1990; Baer 1995), is also a function of the available exposure and hence may only provide a partial understanding. Given these limitations the increasing availability of 3D seismic data provides a powerful tool with which to address such problems. With typical spatial resolutions of 25 m (Yilmaz 2001), such

Fig. 2 Seismic section from the North Rockall Trough with high amplitude doleritic sills marked. *TB* Top Basalt, *BB* base Basalt. Note that the sills do not mirror or match the syn-intrusion surface topography (approx top basalt surface) thus apparently invalidating the compensation models of Bradley (1965) and Roberts (1970). The depth scale is approximate and assumes a seismic velocity of 3 km s^{-1} throughout the entire section. Figure location shown in Fig. 4

Darwin; Fig. 1) as well as smaller centres throughout the basin (Stoker et al. 1993). The Anton Dohrn and Rosemary Bank centres are generally believed to be Late Cretaceous in age with Maastrichian chalks being recovered from their summits (Jones et al. 1974; Morton et al. 1995), but the Darwin centre has to date only provided Palaeocene ages (Tate et al. 1999). Associated with the extrusive igneous material, seismic data suggests an Early Tertiary age for the Rockall Trough sills, with intrusion occurring mainly in the Mesozoic sediments (Fig. 2; Wood et al. 1988).

Methodology

Interpretation of the sill complexes was carried out using two distinct methodologies. Sills were manually picked and mapped in the conventional way after their initial identification on seismic sections on the basis of their tendency to cross-cut stratigraphy and their high seismic amplitudes. This allowed the gross geometry, size and location of sills to be determined along with the geometry of sill-sill contacts (Fig. 3). The sills were then examined using seismic volume visualisation techniques, opacity rendering being the preferred method. This technique provides an effective method with which to study the three-dimensional variability of structural, sedimentary and igneous geology (Kidd 1999) and relies on the conversion of conventional 3D seismic data into a voxel volume. Each voxel contains the information from the original portion of the 3D seismic volume that it occupies, together with an additional user-defined variable that controls its opacity. The opacity of individual voxels can then be varied as a function of their seismic amplitude, allowing the user to examine only those voxels within the volume of interest that fall within a particular amplitude range. The unusually high densities and velocities of doleritic sills (3,000 Kg m^{-3} and 5 km s^{-1}, respectively) combine to give acoustic impedance contrasts commonly in excess of 40% and consequently a higher amplitude seismic reflection compared to a sedimentary body of identical thickness. Consequently, it is relatively easy to make the surrounding country rock transparent whilst preserving all but the thinnest sills as opaque features.

Sill complex geometries

Using a combination of conventional seismic picking and opacity rendering, the seismic data from the North Rockall Trough demonstrate that there are two dominant sill types within the region, both exhibiting complex internal architectures. The common structural form is radially symmetrical and consists of a saucer-like flat inner sill at the base with an arcuate inclined sheet connecting it to a gently inclined, commonly ragged,
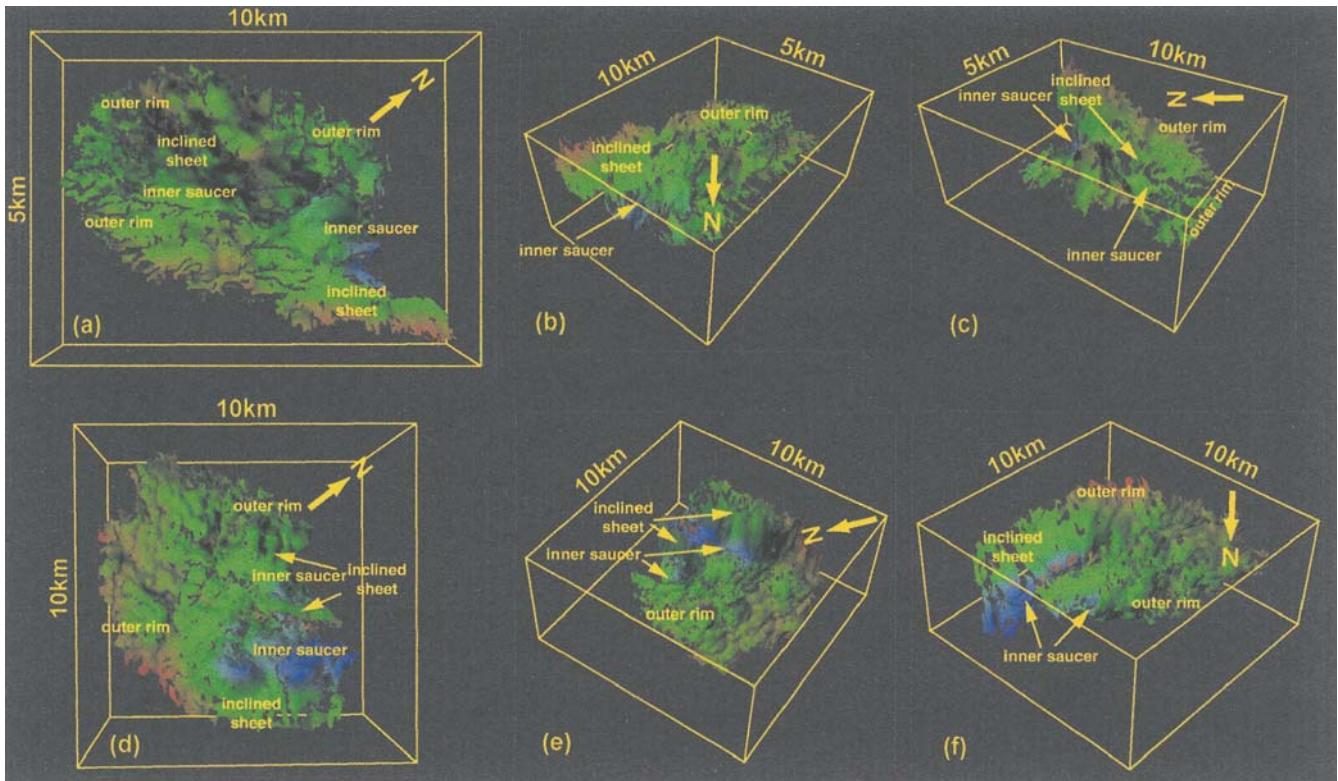

Fig. 3 Artificially illuminated 3D views of hybrid sill complexes produced by mapping the conventionally picked top sill reflector. *Blue colours* represent deeper parts of the sills whilst *green colours* are shallow. **a** and **d** are plan views of **b** and **c** and **e** and **f**, respectively. The locations of the hybrid sill bodies are shown in Fig. 4
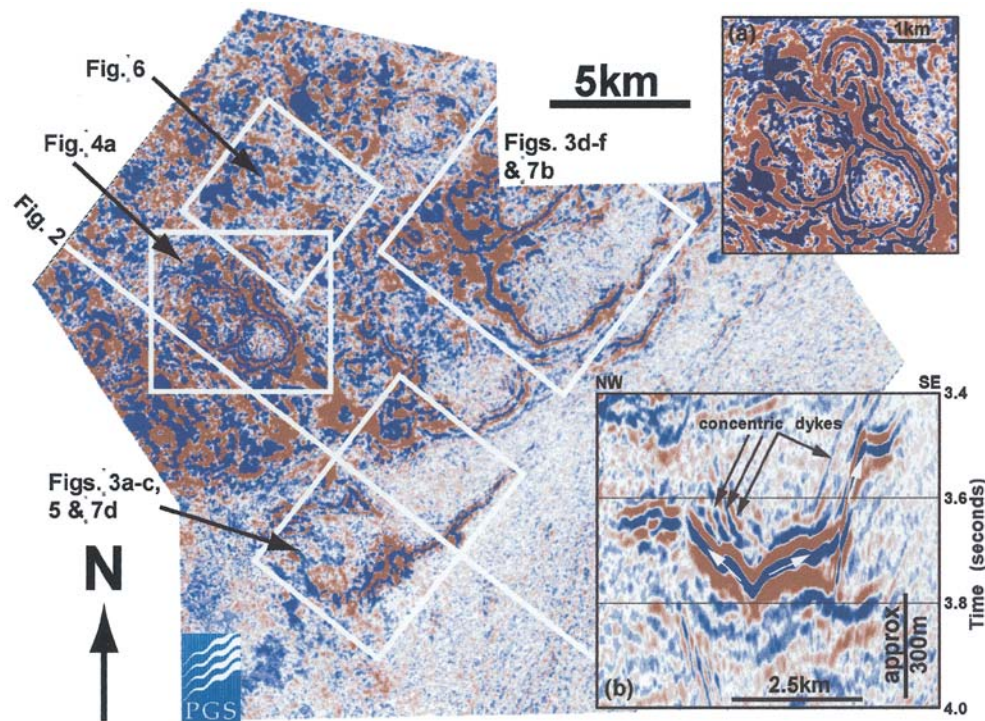
Fig. 4 Travel time slice from the North Rockall Trough 3D seismic. Note the absence of a preferred orientation or elongation direction of the rings and the cuspate geometry of the inclined sheets. **a** Enlargement of part of the image showing the distinctive 'ring-in-ring' pattern due to concentric dyking. **b** seismic section across a typical radially symmetrical sill complex with evidence for multiple concentric dykes rising from the upper surface of the inner saucer producing the distinctive 'ring-in-ring' pattern seen in the travel-time slice. Note the thickest section occurs in middle. Magma flow directions derived from opacity rendering are indicated in *white* (see text for details). The depth scale is approximate and assumes a seismic velocity of 3 km s^{-1} throughout the entire section. For location see Fig. 5

outer rim (Figs. 3 and 4). Such geometries previously have been documented using 3D seismic data from the Faeroe-Shetland Basin (Davies et al. 2002; Smallwood and Maresh 2002) and in classic onshore localities such as the Karoo of South Africa (Du Toit 1920; Chevalier and Woodford 1999), the Whin Sill (Francis 1982; Johnson and Dunham 2001), the Midland Valley Sill (Francis 1982) and in Tasmania (Leaman 1975). The largest sills in the North Rockall Trough displaying this geometry are roughly radially symmetrical and approximately 5 km wide (cf. Chevalier and Woodford 1999). They appear to form the fundamental building blocks for sill intrusion across the region and consequently will be referred to as sill complexes whilst the term sill will refer to smaller units of the sill complex. Rising from the upper surface of each inner saucer, a number of thin concentric dykes can be observed (Fig. 4), producing the distinctive 'ring-in-ring' pattern previously documented for the Karoo sills (Chevalier and Woodford 1999; Fig. 4). Within a sill complex the seismic data also demonstrate that the inclined sheet consists of a series of concave inwards segments providing the cuspate geometry also seen in the Karoo sills (Chevalier and Woodford 1999; Fig. 4). Such sill complexes can appear as isolated bodies but commonly occur in close proximity to each other and consequently merge to produce hybrid geometries in-

volving multiple inner saucers, inclined sheets and outer rims (Fig. 3).

Figure 5 is a 3D volume visualisation of the hybrid sill complex shown in Fig. 3a–c in which the country rock has been made transparent. Each sill complex consists of a thick inner saucer connected by an inclined sheet to an outer rim of variable thickness. However, further details of the internal structure also can be seen. The inclined sheet, generally the thinnest part of the sill complex, contains thicker linear regions radially distributed around the inner saucer. From these linear thickenings, smaller scale linear features can be seen branching off to form a dendritic network that extends from the periphery of the inner saucer through the inclined sheet to the outer rim. These branching relationships are interpreted as magma flow channels within the sheet. As the branches always terminate towards the sill periphery and can be traced back through parent channels to the inner saucer, the sill complexes are interpreted to grow radially outwards from the inner saucer. This implies that the sill complexes consist of a series of primary flow units rising from the inner saucer and radiating outwards and upwards. With an average length of around 3 km, and a width of 1 km, each primary flow unit is fed by a primary magma tube, generally elongated in the direction of propagation (i.e. towards the sill complex periphery) and has a slightly

concave upwards cross section normal to the direction of propagation (Fig. 5). This latter geometry accounts for the cuspate geometry of the inclined sheets (Fig. 4). Primary magma tubes bud to form secondary magma tubes that feed secondary flow units with average lengths of around 1–2 km and widths of 0.5–1 km. Secondary flow units propagate at an angle of approximately 45 ° to their parent primary magma tube flow/propagation direction (Fig. 5). As with primary flow units, secondary flow units also display a slightly concave upwards cross section. Secondary flow units derived from the same primary flow unit are generally sub-parallel. This pattern of subdividing flow units is replicated down to scales of approximately 100 m, with successively smaller flow units being fed from magma tubes repeatedly branching from higher order tubes (Fig. 5).

Elongate, bilaterally symmetrical sill complexes also can be found within the North Rockall Trough. Unlike the radially symmetrical sill complexes, these bodies are in close proximity and likely directly related to overlying volcanoes (Fig. 6). They occur as a series of radiating sills originating from beneath the volcano or from the periphery of the ring fault/dyke underlying the volcano. Their geometric form is an elongate, concave upwards trough, similar in general form to the primary and secondary flow units seen in radially symmetrical sill complexes. With a general tendency to climb away from their magma source, these elongate sill complexes also branch as they propagate, with individual buds (or flow units) also having a general concave upwards profile.

Fig. 5 a Plan view of a 3D seismic volume containing a hybrid sill complex in which the low amplitude 'country rock' has been made transparent. For location see Fig. 4. The *rendered colours* are a function of seismic amplitude (*blue* higher, *brown* lower amplitude). The artificially illuminated plan view of the hybrid sill complex used in **b** is also shown for ease of comparison (c.f. Fig. 3a). The *rendered pattern* illustrates the branching nature of sill complexes sourced from two thick inner saucers. The area to the north of the *blue dashed line* contains rendered material lying above the hybrid sill body and consequently can be ignored. The area to the west of the *red dashed line* contains a rendered sill body lying below the hybrid sill body of interest. This deeper sill body shows east–west-trending lineations. These are interpreted to be magma tubes that connect with, and feed, the eastern inner saucer of the shallow hybrid sill complex. This feeder relationship is also shown in Fig. 10d. **b** artificially illuminated plan view of the hybrid sill complex in **a**. The *yellow lines* mark the inferred position of the magma tubes with *arrowheads* indicating the flow directions. The *dashed lines* mark the limits of primary flow units. The *red lines* mark the orientation of the magma tubes in the deeper sill complex with the *arrowheads* showing inferred magma flow directions. The *numbered white arrows* indicate the locations of seismic sections with the number indicating the figure in which they can be found. **c** 3D seismic volume image of part of a primary flow unit within the hybrid sill complex shown in **a**. Secondary magma tubes, feeding secondary flow units, can be seen branching from the primary magma tube. Secondary flow units can also be seen to subdivide into lower order (tertiary) flow units
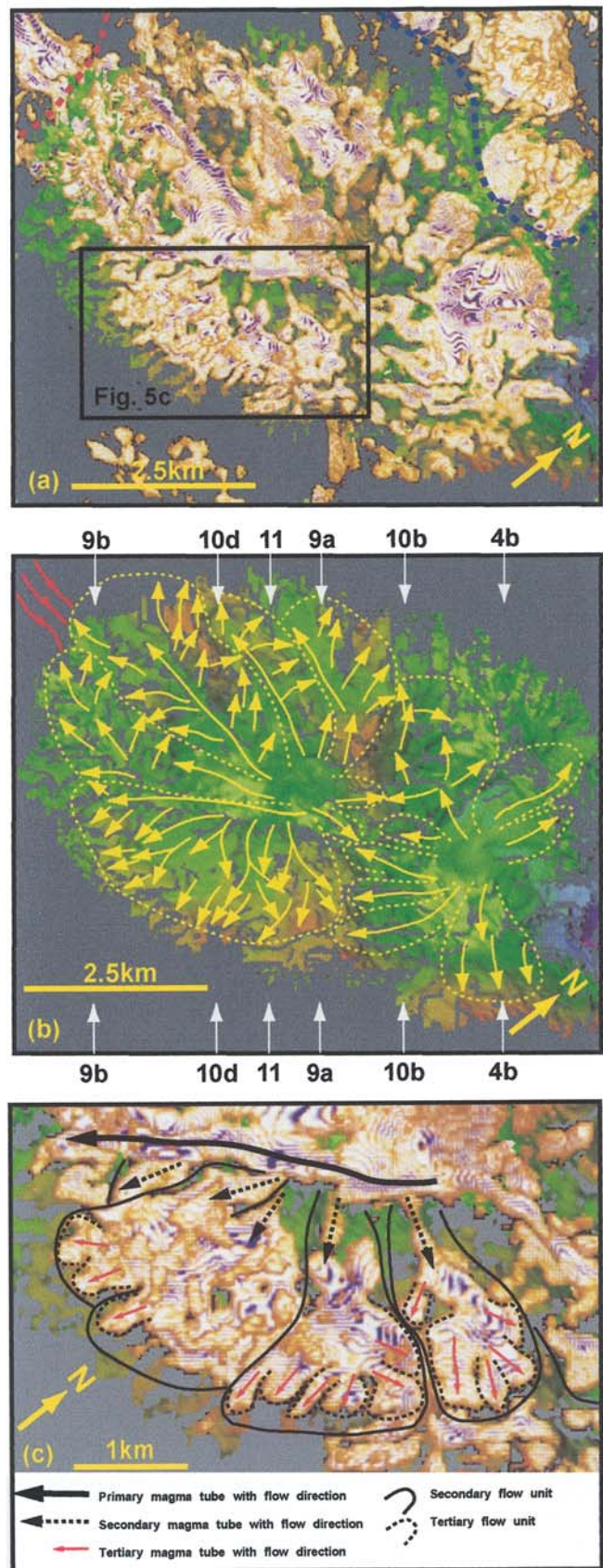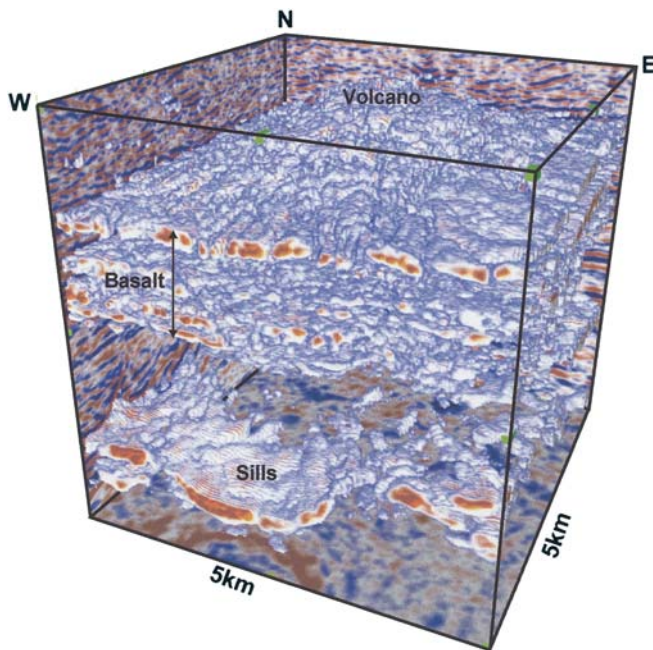
Fig. 6 3D opacity rendered image of a volcano within the North Rockall Trough and the underlying concave upwards, trough-like, sill complexes beneath it. The *rendered colours* are a function of seismic amplitude (*brown* higher, *blue* lower amplitude). In order to make the limits of the volume more readily recognisable the north-western and north-eastern walls contain conventional seismic sections. Similarly, the volume floor contains a travel-time slice. For location see Fig. 4

Sill merger and the development of junctions

The merging of sill complexes to form hybrid sill complexes, or the merger of flow units within a sill complex, results in the development of junctions due to the abutment of a sill or sill complex against a second sill or sill complex.

Merging sill complexes to form hybrid sill complexes usually results in the development of inclined and antiformal junctions. The inclined junction develops due to the abutment of an inclined sheet against another inclined sheet of an adjacent sill complex (Fig. 7). As the inclined sheet terminates against the second sill complex that part of the sill complex will not develop an outer rim. The second sill complex can be fully developed unless it too terminates against another sill complex (Fig. 7). The entire boundary between the two sill complexes can be an inclined junction but in some circumstances an inclined junction can gradually transform into an antiformal junction. Antiformal junctions develop between the tips of two inclined sheets from adjacent sill complexes. Unlike inclined junctions, both of the inclined sheets are equally developed and merge to form a tight antiformal closure with neither inclined sheet continuing upwards to form an outer rim (Fig. 7). This form appears to correspond to the tight ridges described by Spry (1958) that connect saucers in the Tasmanian sills and the antiformal closures observed in the Karoo (Du Toit 1920).

Both sill complexes connected by an antiformal junction lack peripheral outer rims along the length of the antiformal junction as the inclined sheets mutually terminate. Tight antiformal junctions and inclined junctions develop when the inner saucer separation between adjacent sill complexes is relatively large (>2 km), but broader, open antiformal junctions can also be found between sill complexes with smaller inner saucer separations. This form develops due to the merger of the gently dipping lower parts of the inclined sheets close to their parent inner saucers. Other merging geometries involving the abutment of an inner saucer or outer rim with an inclined sheet also can be observed, with the merged sill complexes forming distinctive 'T' or 'F'-shaped geometries in the area of merger (Fig. 8).

The most complex merging geometries occur between the outer rims of adjacent sill complexes, presumably as a consequence of the complex ragged nature of the outer rims, or between flow units within a sill complex. The common forms of junctions seen in such regions correspond to the bridges described for dykes by Rickwood (1990). In most circumstances a partial bridge develops with one flow unit terminating on an adjacent flow unit (Fig. 9). However, the two flow units can on occasion mutually terminate against each other to form a broken bridge, this being an isolated block of country rock enveloped by the merging sill units (Fig. 9).

Flow indicator structures within sill complexes

Although junctions mark the limits of flow units within both simple sill complexes and hybrid sill complexes, a number of structures can be found within sill complexes that place constraints on magma flow directions. Steps are vertical offsets, or dyke-like connections, between two sub-parallel sill segments emplaced at slightly different stratigraphic levels (Fig. 10; Francis 1982; Rickwood 1990). The sill segments can be traced back to a larger sill emplaced at a single stratigraphic level and are only observed between sills originating from the same parent sill body. In some circumstances the sub-parallel sill segments form a series of separate bodies in an en-echelon pattern (Fig. 10). The 'step and stair' morphology of sills (Francis 1982; Rickwood 1990) and the 'fingers' of Pollard et al. (1975) all appear to be different terms used to describe the same geometries discussed in this paper and have traditionally been interpreted as flow parallel features. With the aid of opacity rendering, the above features can be readily explained by the budding of new lower order magma tubes within a higher order magma flow unit. These lower order magma tubes feed lower order magma flow units that are approximately sub-parallel to each other and propagate at an angle of approximately 45° to the propagation direction of the parent body, with small variations in the level of their emplacement. Consequently, the orientation of steps and sill fingers/flow units and the direction of branching
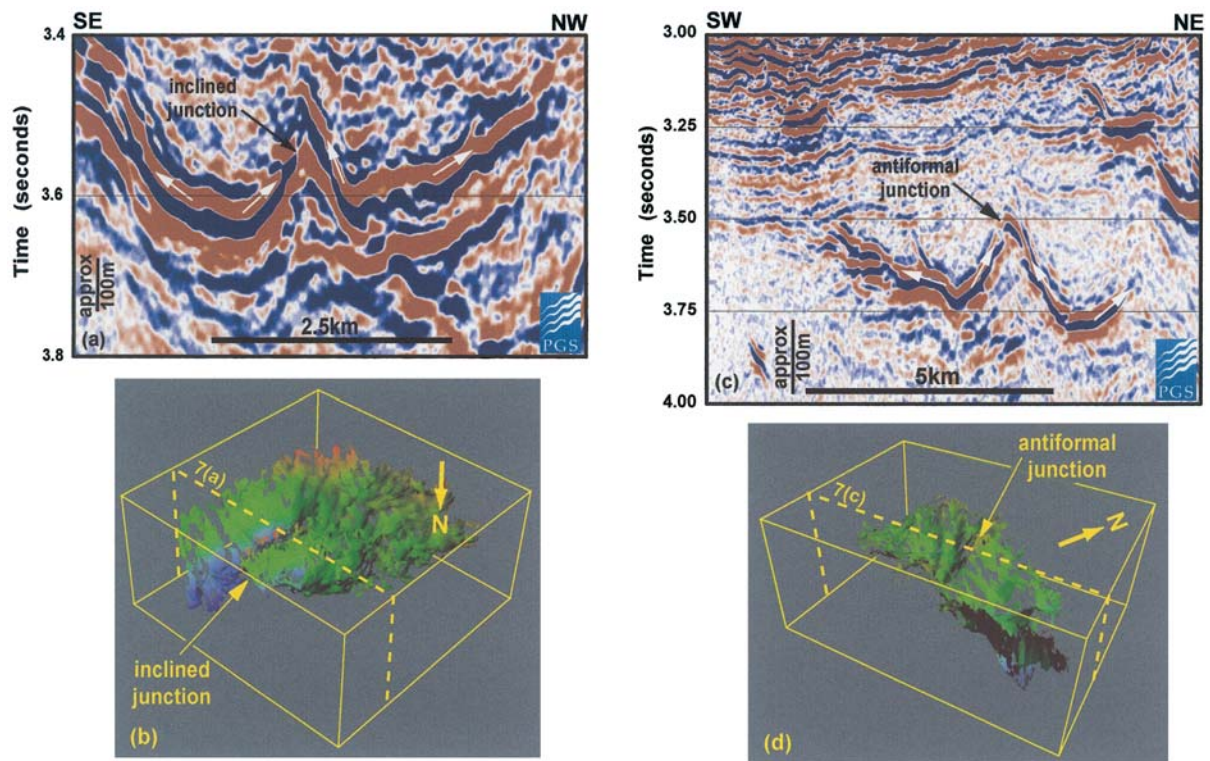
Fig. 7 a Seismic section showing an inclined junction linking two sill complexes with the sill on the left terminating against the sill on the right. Magma flow directions derived from opacity rendering are indicated in *white* (see text for details). The depth scale is approximate and assumes a seismic velocity of 3 km s^{-1} throughout the entire section. **b** 3D view of a hybrid sill complex involving an inclined junction (cf. Fig. 3) and the location of the seismic section shown in **a**. **c** seismic section showing an antiformal junction linking two sill complexes. Magma flow directions derived from opacity rendering are indicated in *white* (see text for details). The depth scale is approximate and assumes a seismic velocity of 3 km s^{-1} throughout the entire section. **d** 3D view of a hybrid sill complex involving an antiformal junction (cf. Fig. 3) and the location of the seismic section shown in **c**. The locations of the 3D views (**b** and **d**) are shown in Fig. 4
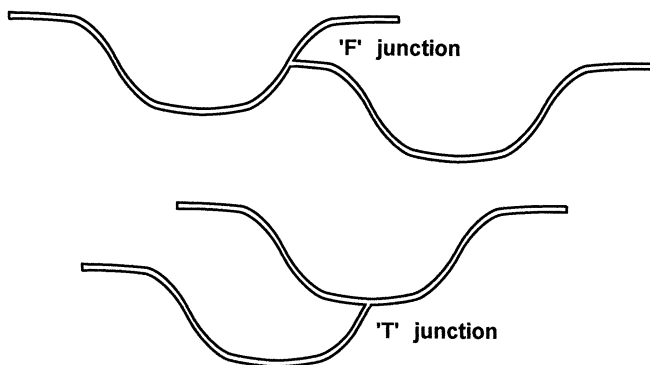

Fig. 8 Schematic illustrations of potential junction geometries involving inclined sheets connecting with inner saucers or outer rims

within a sill complex provide primary evidence for the flow direction within that part of the complex.

Failed attempts at budding new subsidiary flow units result in the development of "horns", which are elongate sheet-like protrusions forming at an angle of approximately 45° to their parent sill which can be found along the base and flanks of sills (Fig. 11). Such features are interpreted to be the preserved remnants of embryonic magma tubes and, like stepped/en echelon fingers, propagate at an angle of approximately 45° to the propagation direction of the parent body. These have previously been recognised in the field for both sills and dykes (Pollard and Johnson 1973; Francis 1982; Rickwood 1990). Consequently, the directions in which horns terminate provide evidence for the flow direction within the parent flow unit, consistent with previous observations in the field (Fig. 11; Bradley 1965; Grapes et al. 1972; Francis 1982). Rising from the upper surface of each inner saucer, a number of thin concentric dykes can also be observed (Fig. 4); producing the distinctive 'ring-in-ring' pattern previously documented for the Karoo sills (Chevalier and Woodford 1999). Both the concentric dykes and the inclined sheets can be shown to climb and terminate in the inferred direction of magma flow within the region of the sill complex from which they originate (Fig. 4). Concentric dykes rising from the upper surface of sill complexes have previously been interpreted as intruded tensional fractures developing ahead of a propagating sill (Bradley 1965; Grapes et al. 1972).
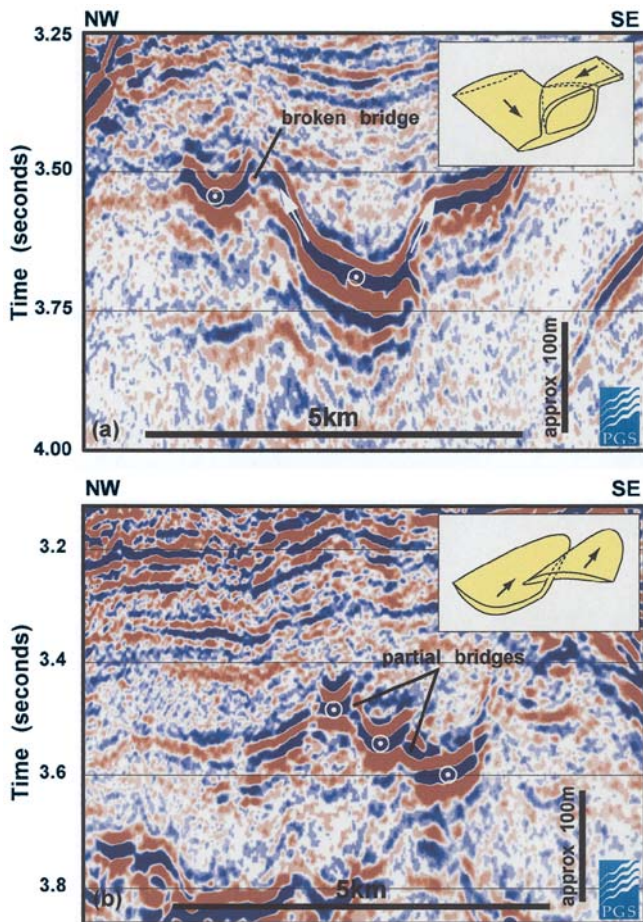
Fig. 9 a Seismic section (and cartoon) of a broken bridge formed by the merger of two flow units converging at approximately 90 within a sill complex. Magma flow directions derived from opacity rendering are indicated in *white*, with *circles* indicating a flow normal to the page (see text for details). **b** seismic section (and cartoon) of a partial bridge formed by the merger of parallel flow units within a sill complex. Magma flow directions derived from opacity rendering are indicated in *white* (see text for details). The depth scales are approximate and assume a seismic velocity of 3 km s^{-1} throughout the entire section. Seismic section locations shown in Fig. 5

Models for sill emplacement

The data from the North Rockall Trough suggests that each radially symmetrical sill complex is independently fed from a source underlying the inner saucer. Apart from Leaman (1975), the majority of outcrop-based studies on sill intrusion have suggested that sills are dyke sourced. Consequently, one would expect an alignment of sill complexes corresponding to the preferred dyke orientation across the region (Francis 1982; Chevalier and Woodford 1999; Johnson and Dunham 2001). However, evidence for dykes feeding sills is often lacking (e.g. Johnson and Dunham 2001). As typical seismic acquisition and processing techniques are not designed to image steeply dipping features such as dykes, the North Rockall Trough dataset provides no direct evidence for the

number or orientation of dykes within the study area. In the current example there is no linear alignment of the saucer shaped sill complexes (Fig. 4). Furthermore, Fig. 10d clearly shows the inclined sheet of a deep hybrid sill complex merging with the inner saucer of a shallower hybrid sill complex. This geometry is consistent with the idea that the shallow hybrid sill complex is sourced from the deeper hybrid sill complex and that the feeder is located at the centre (deepest part) of the inner saucer of the shallow complex. This feeder relationship is consistent with the observed radial and branching magma flow shown in Fig. 5 and the presence of deeper magma tubes shown in the same figure. The data imply that the sill complexes grow by climbing from the centre outwards. Such an observation does not fit easily with the majority of existing models of sill emplacement, as most of these have the feeders located at the periphery of the sill complexes, with magma intruding both upwards and downwards (Francis 1982; Francis and Walker 1986; Chevalier and Woodford 1999).

Four basic mechanisms for doleritic sill intrusion have been proposed, largely based on outcrop studies. The concept of "compensation", as proposed by Bradley (1965), suggests that sills intrude at depths where the magma pressure equals the lithostatic pressure. Upon reaching the compensation level, an ascending dyke will intrude along the compensation level, with both upwards and downwards magma propagation possible. Bradley (1965) proposed that this mechanism of intrusion would result in sills forming a mirror image of the overlying topography (Fig. 12a). To date, testing this mechanism has been problematic as the syn-intrusion topographic surface is difficult to constrain in eroded outcrop settings. However, Fig. 2 demonstrates that the geometry of the Palaeogene sills intruded into the North Rockall Trough bears no relationship to the top basalt surface, which is a close approximation to the contemporaneous surface at the time of intrusion. Furthermore, the necessity for the model to involve downward as well as upward magma flow suggests that this model is incompatible with the observations. A second variant on the concept of compensation was proposed by Roberts (1970), with sill intrusion parallel to the topography. Again, Fig. 2 demonstrates that such a relationship does not exist for the sills within the North Rockall Trough.

The development of the Whin and Midland Valley sills, northern Britain, has been explained by Francis (1982) using the concepts of magma overshoot and gravitational flow. In this model an ascending feeder dyke overshoots the optimum level for lateral intrusion (cf. Bradley 1965). As the magma is at too high a level and is denser than the surrounding country rock, it flows laterally downwards and accumulates in the basin floor. The descent exploits bedding where possible but regularly transgresses downwards. As magma accumulates on the basin floor, the forces attempting to re-establish hydrostatic equilibrium drive magma from the basin floor upwards on the opposite side of the basin so that the full dish is developed (Fig. 12b). When applied to the North
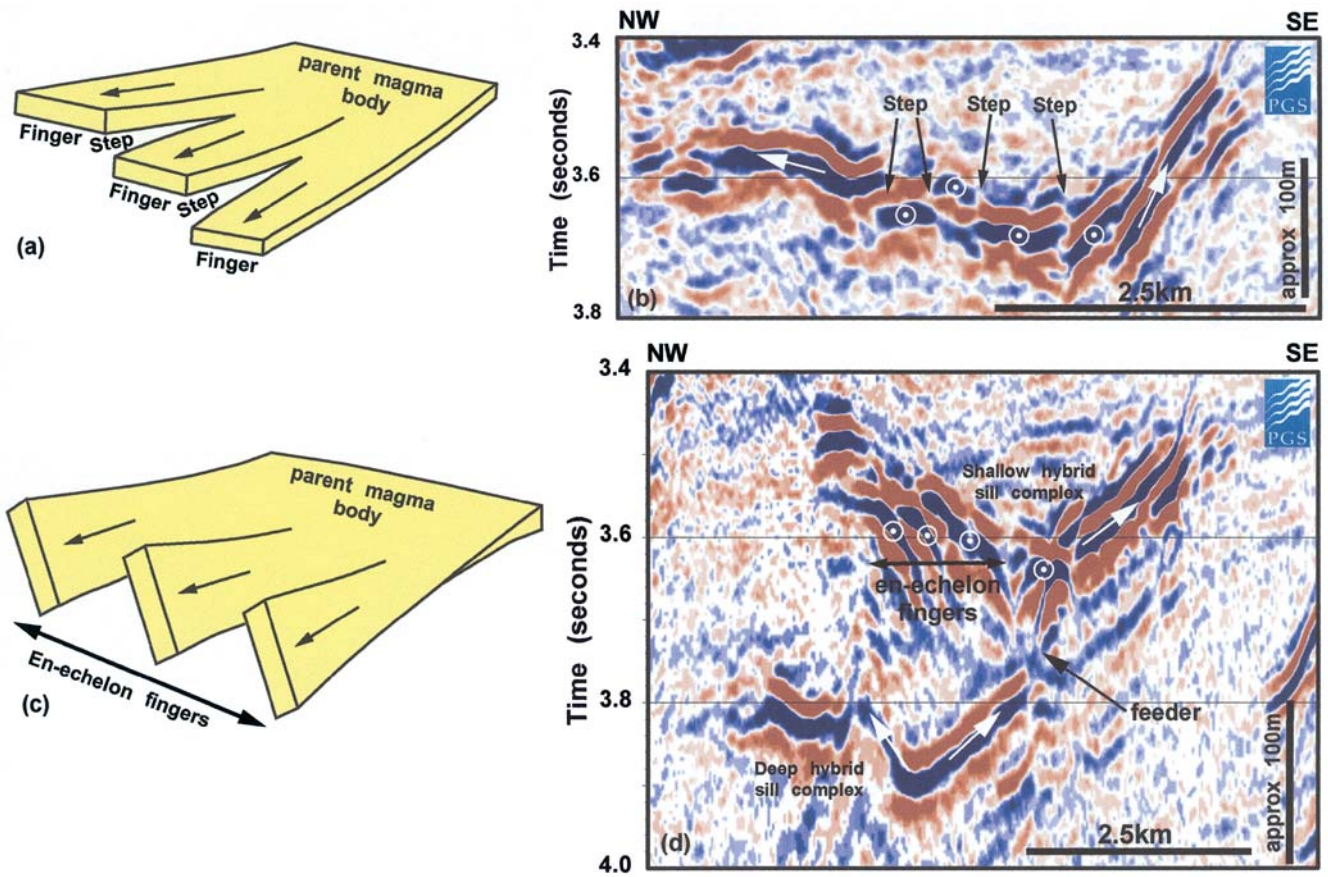
Fig. 10 a Cartoon of stepped sill fingers and their relationship to the parent sill. *Arrows* indicate flow directions. **b** seismic section of stepped sill fingers. Magma flow directions derived from opacity rendering are indicated in *white*, with *circles* indicating a flow normal to the page (see text for details). The depth scale is approximate and assumes a seismic velocity of 3 km s^{-1} throughout the entire section. **c** cartoon of en echelon sill fingers and their relationship to the parent sill. *Arrows* indicate flow directions. **d** seismic section of en echelon sill fingers. Magma flow directions derived from opacity rendering are indicated in *white*, with *circles* indicating a flow normal to the page (see text for details). The section also shows a deep hybrid sill complex terminating at the base of the shallow hybrid sill complex. As the flow within the shallow hybrid sill complex can be shown to originate from the region where the deep hybrid sill complex terminates, this implies that the deeper hybrid sill complex fed the shallow hybrid sill complex. The depth scale is approximate and assumes a seismic velocity of 3 km s^{-1} throughout the entire section. Seismic section locations shown in Fig. 5
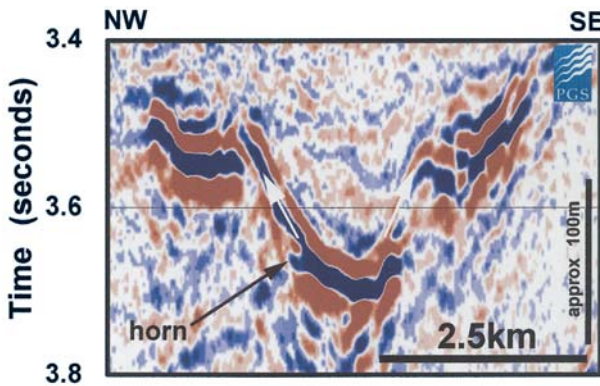

Fig. 11 Seismic section showing a horn with magma flow directions derived from opacity rendering indicated in *white* (see text for details). The depth scale is approximate and assumes a seismic velocity of 3 km s^{-1} throughout the entire section. Location shown in Fig. 5

Rockall Trough sills, this models fails as it requires laterally offset feeders and downwards magma flow.

The ring dyke model of Chevalier and Woodford (1999) suggests that an ascending ring dyke begins to develop a flatter outer rim, with its inflation gradually lifting the country rock overlying the ring dyke. Uplift of the block subsequently allows the downward migration of magma into the area contained within the ring dyke, leading to the development of a flat inner sill within the confines of the ring dyke (Fig. 12c). This model, developed for the Karoo sills, cannot account for the radial upward and outward, flow observed within the North Rockall Trough.

Burger et al. (1981) proposed that the emplacement of the Karoo sills could be explained using the model of Pollard and Johnson (1973) developed for the diorite sills and laccoliths of the Henry Mountains, Utah. The model assumes that the sill overlies a central feeder and that the inner saucer thickens sufficiently to result in roof uplift

Fig. 12 Models for radially symmetrical sill growth. **a** The concept of a compensation surface mirroring topography (Bradley 1965). **b** magma overshoot and gravitational flow (Francis 1982). **c** the ring dyke model (Chevalier and Woodford 1999). **d** this study and Burger et al. (1981): are centrally sourced laccolith model with peripheral dyking. **e** model for volcano related, bilaterally symmetrical, sills based on **d**
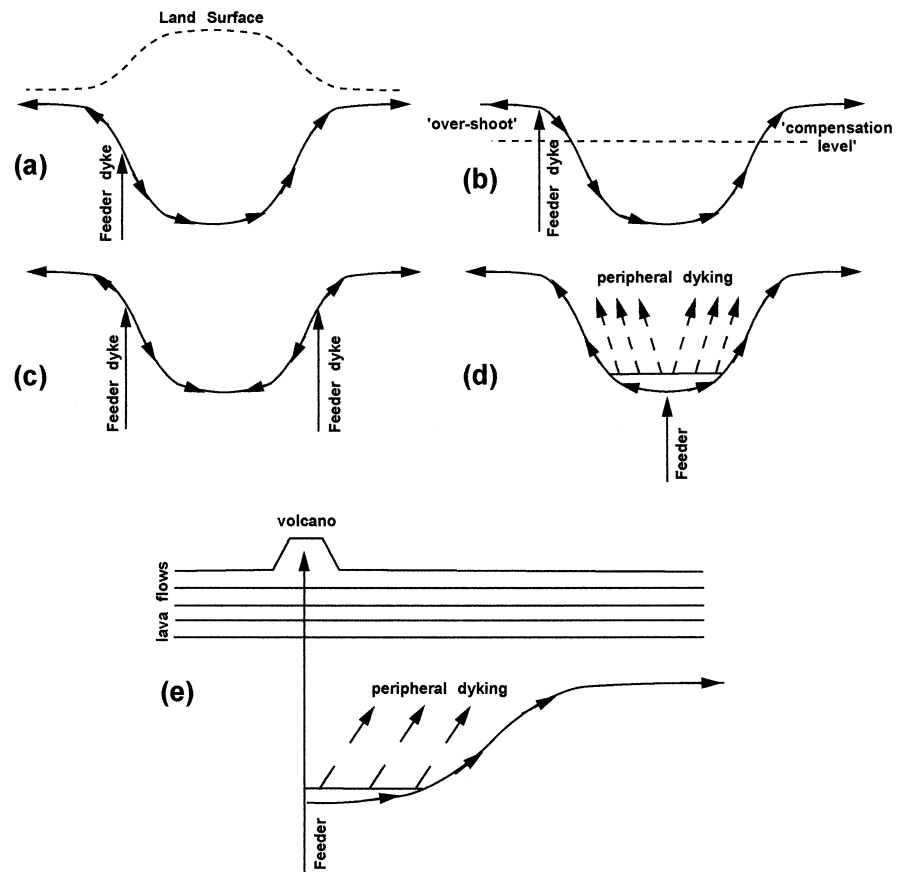
and radial peripheral fracturing and dyking. This allows the development of inclined sheets that propagate upwards until they develop into flatter outer rims (Fig. 12d). Such a model is most compatible with the observations from the North Rockall Trough. The thicker inner saucers imaged seismically (Fig. 4), the development of concentric dykes to produce the 'ring-in-ring' pattern, and the inclined sheets at the periphery of the inner saucer can be interpreted as attempts to exploit concentric radial peripheral fractures developed during roof uplift associated with the growth of the inner saucer. The radiating flow and proposed central feeders required by the North Rockall Trough data also appear to be compatible with this model. However, Chevalier and Woodford (1999) suggested that the doleritic Karoo sills do not have the correct inner saucer thickness-length ratios or evidence for central feeders required by the model.

As the general morphology of bilaterally symmetrical sills is broadly similar to that of flow units within radially symmetrical sills, and as their internal architectures are essentially the same (e.g. lobes and branching), this would suggest their growth and emplacement mechanisms must share some common controls. However, bilaterally symmetrical sills lack the underlying central source seen in radially symmetrical sill complexes. Our model instead begins with the diversion of magma destined for eruption and its lateral injection into the country rock beneath the

volcano (Fig. 12e). If this continues, then the growing sill will thicken gradually in a manner similar to that proposed for the inner saucers of the radially symmetrical sills, with peripheral dyking and continued lateral intrusion (Fig. 12e). Such lateral sill growth and peripheral dyking would eventually result in the development of inclined sheets, leading to the gradual climbing of the sill away from the magma source from which it originated. Furthermore, peripheral dyking on the flanks of the intrusion would allow the development of the concave upwards, trough-like, cross section by the same mechanism.

Conclusions

Examples of sill complexes in the North Rockall Trough occur as either radially or bilaterally symmetrical forms. Radially symmetrical sill complexes consist of a saucer-like inner sill at the base with an arcuate inclined sheet connecting it to a gently inclined, commonly ragged, outer rim and are approximately 5 km wide. The inclined sheet consists of a series of concave inwards segments (flow units) producing the distinctive cuspate geometry previously noted for the Karoo sills. Bilaterally symmetrical sill complexes are in close proximity to and are directly sourced by magma feeding an overlying volcano. They have an elongate, concave upwards, trough-like

geometry and climb away from the magma source from which they are fed. Both radially and bilaterally symmetric sill complexes can appear as isolated bodies but commonly occur in close proximity and consequently merge, producing hybrid sill complexes involving multiple inner dishes, inclined sheets and outer rims.

Radially symmetrical sill complexes consist of a series of radiating primary flow units rising from the inner saucer which are fed by primary magma tubes. Such flow units contain smaller scale secondary flow units, each being fed by a secondary magma tube branching from the primary magma tube. Similarly, bilaterally symmetrical sill complexes show a hierarchy of flow units which branch in the direction of sill propagation. This radiating and branching flow pattern, as well as the interaction between flow units of varying orders, provides new insights into the origin of the structures commonly seen within sill complexes and the hybrid sill bodies produced by their merger. Rising from the upper surface of each inner saucer, a number of thin, concentric dykes are observed that climb in the direction of magma flow within the region of the sill complex from which they originate; such dykes produce the distinctive 'ring-in-ring' pattern previously documented for the Karoo sills.

The data suggest the following conclusions: (1) magma flow in sills may occur in channels; (2) each radially symmetrical sill complex is fed independently from an underlying centrally located source; (3) sills grow by climbing from the centre outwards; (4) growth is associated with peripheral fracturing and ring dyking. The only published model for sill emplacement that appears compatible with the observations is a laccolith style model similar to that for the diorite intrusions of the Henry Mountains, Utah (Pollard and Johnson 1973). Bilaterally symmetrical sill complexes are elongate features that are sourced from one end (the magma conduit feeding the overlying volcano). However, the flow of magma, with its branching hierarchy of flow units, is broadly similar to that of the radially symmetrical sill complexes, suggesting that the general features of the laccolith emplacement model also apply to bilaterally symmetrical sill complexes.

References

Baer G (1995) Fracture propagation and magma flow in segmented dykes: field evidence and fabric analyses, Makhtesh Ramon, Israel. In: Baer G, Heimann A (eds) Physics and chemistry of dykes. Balkema, Rotterdam, pp 125–140

Bradley J (1965) Intrusion of major dolerite sills. Trans R Soc NZ 3:27–55

Burger CAJ, Hodgson FDI, Van der Linde PJ (1981). Hidroliese eienskappe van akwifere in die Suid-Vrystaat. Die ontwikkeling en evaluering van tegnieke vir die bepaling van die ontginninspotensiaal van grondwaterbronne in die Suid-Vrystraat en in Noord-Kaapland. Inst. Groundwater Stud., Univ. Orange Free State, Bloemfontein, South Africa. 2:115

Chevalier L, Woodford A (1999) Morph-tectonics and mechanism of emplacement of the dolerite rings and sills of the western Karoo, South Africa. S Afr J Geol 102:43–54

Davies R, Bell BR, Cartwright JA, Shoulders S (2002) Three-dimensional seismic imaging of Paleogene dike-fed submarine volcanoes from the northeast Atlantic margin. Geology 30:223–226

Du Toit AL (1920) The Karoo dolerite of South Africa: a study of hypabyssal injection. Trans Geol Soc S Afr 23:1–42

Francis EH (1982) Magma and sediment-I. Emplacement mechanism of late Carboniferous tholeiite sills in northern Britain. J Geol Soc Lond 139:1–20

Francis EH, Walker BH (1986) Emplacement of alkali-dolerite sills relative to extrusive volcanism and sedimentary basins in the Carboniferous of Fife, Scotland. Trans R Soc Edinb 77:309–323

Grapes RH, Reid DL, McPherson JG (1972) Shallow dolerite intrusion and phreatic eruption in the Allan Hills region, Antarctica. NZ J Geol Geophys 17:563–577

Hitchen K, Ritchie JD (1993) New K-Ar ages, and a provisional chronology, for the offshore part of the British Tertiary Igneous Province. Scott J Geol 29:73–85

Johnson GAL, Dunham KC (2001) Emplacement of the Great Whin Dolerite Complex and the Little Whin Sill in relation to the structure of Northern England. Proc Yorkshire Geol Soc 53:177–186

Jones EJW, Ramsay ATS, Preston NJ, Smith ACS (1974) A cretaceous guyot in the Rockall Trough. Nature 251:129–131

Kidd GD (1999) Fundamentals of 3D seismic volume visualization. Leading Edge 18:702–709

Leaman DE (1975) Form, mechanism, and control of dolerite intrusion near Hobart, Tasmania. J Geol Soc Aust 22:175–186

Morton AC, Hitchen K, Ritchie JD, Hine NM, Whitehouse M, Carter SG (1995) Late cretaceous basalts from Rosemary Bank, northern Rockall Trough. J Geol Soc Lond 152:947–952

Mussett AE, Dagley P, Skelhorn RR (1988) Time and duration of activity in the British Tertiary Volcanic Province. In: Morton AC, Parson LM (eds) Early Tertiary volcanism and opening of the NE Atlantic. Geol Soc Lond Spec Pub 39:337–348

Pollard DD, Johnson AM (1973) Mechanics of growth of some laccolith intrusions in the Henry Mountains, Utah, Part II. Tectonophysics 18:311–354

Pollard DD, Muller OH, Dockstader DR (1975) The form and growth of fingered sheet intrusions. Geol Soc Am Bull 86:351–363

Rickwood PC (1990) The anatomy of a dyke and the determination of propagation and magma flow. In: Parker AJ, Rickwood PC, Tucker DH (eds) Mafic dykes and emplacement mechanisms. Balkema, Rotterdam, pp 81–100

Roberts JR (1970) The intrusion of magma into brittle rocks. In: Newall G, Rast N (eds) Mechanism of igneous intrusion. Geol J Spec Issue 2, p 380

Smallwood JR, Maresh J (2002) The properties, morphology and distribution of igneous sills: modelling, borehole data and 3D seismic data from the Faeroe-Shetland area. In: Jolley DW, Bell BR (eds) The North Atlantic Igneous Province: Stratigraphy, tectonic, volcanic and magmatic processes. Geol Soc Lond Spec Pub 197:271–306

Smythe DK (1989) Rockall Trough—Cretaceous or Late Palaeozoic? Scott J Geol 25:5–43

Spry AH (1958) Some observations of the Jurassic dolerite of the Eureka cone sheet near Zeehan, Tasmania. In: Dolerite: a symposium. Hobart University, Tasmania, pp 93–129

Stoker MS, Hitchen K, Graham CC (1993) The geology of the Hebridies and west Shetland Shelves, and adjacent deep water

areas. United Kingdom Offshore Regional Report, Br Geol Surv Lond, 149 pp

Tate MP, Dodd CD, Grant NT (1999) The Northeast Rockall Basin and its significance in the evolution of the Rockall-Faeroes/East Greenland rift system. In: Fleet AJ, Boldy SAR (eds) Petroleum geology of Northwest Europe: Proceedings of the 5th Conference. Geol Soc Lond, pp 391–406

Upton BGJ (1988) History of Tertiary igneous activity in the North Atlantic borderlands. In: Morton AC, Parsons LM (eds) Early Tertiary volcanism and the opening of the NE Atlantic. Geol Soc Lond Spec Publ 39:429–454

White RS (1988) A hot-spot model for early Tertiary volcanism in the N Atlantic. In: Morton AC, Parsons LM (eds) Early Tertiary

volcanism and the opening of the NE Atlantic. Geol Soc Lond Special Publ 39:3–13

White RS, McKenzie D (1989) Magmatism at rift zones: the generation of volcanic continental margins and flood basalts. J Geophys Res 94:7685–7729

Wood MV, Hall J, Doody JJ (1988) Distribution of early Tertiary lavas in the NE Rockall Trough. In: Morton AC, Parsons LM (eds) Early Tertiary volcanism and the opening of the NE Atlantic. Geol Soc Lond Spec Publ 39:283–292

Yilmaz Ö (2001) Seismic data analysis processing, inversion and interpretation of seismic data. Soc Explor Geophys Tulsa, 2,027 pp